J. Opt. A: Pure Appl. Opt. **11** (2009) 114018 (8pp) doi:10.1088/1464-4258/11/11/114018

Metamaterial-induced band-gap of surface plasmon propagation

E Popov, S Enoch and N Bonod

Institut Fresnel, Aix-Marseille Université, CNRS, Faculté St-Jérôme,
13397 Marseille Cedex 20, France

E-mail: e.popov@fresnel.fr

Received 28 January 2009, accepted for publication 27 March 2009
Published 16 September 2009
Online at stacks.iop.org/JOptA/11/114018

Abstract
Surface plasmon propagation along a periodically corrugated metallic–air interface can be completely suppressed due to the formation of an equivalent dielectric metamaterial layer with a large real part of its effective refractive index. The effect can be explained by the transformation of the surface plasmon excitation conditions into a Brewster effect. This phenomenon leads to a high absorption of the incident light over a very wide range of incidence. One-dimensional periodicity (classical grating) leads to a single-polarization absorption, while two-dimensional periodicity (crossed grating) results in omnidirectional absorption in unpolarized light.

Keywords: surface plasmon band-gap, total light absorption, diffraction gratings

1. Introduction

Historically, the studies of surface plasmons on corrugated metallic surfaces can be divided into several periods. The first one started with the discovery by Wood [1] of the diffraction efficiency anomaly of classical metallic gratings, and finished with the work of Fano [2] that linked Wood's anomaly to surface plasmon excitation. The second period contained research in two main directions. The first aim was to understand better the role of the surface plasmon excitation in the formation of efficiency anomalies [3] and to reduce the anomalies, because of their devastating effects for spectral instrument performance. The second direction consisted in increasing the strong resonant absorption for the needs of photovoltaics and optical detection. The turning point was the discovery of total light absorption by shallow gratings with one- or two-dimensional periodicity (classical [4] or crossed [5] sinusoidal gratings). While classical gratings can support surface plasmons in only one (TM—transverse magnetic) polarization, crossed gratings can excite them in two perpendicular directions, thus permitting total absorption in unpolarized light. Later, it was shown that a similar effect can appear in deep sinusoidal gratings and in grazing incidence [6, 7]. The third period started with the work of Ebbesen *et al* [8], which attracted the attention of much larger part of the scientific community. The explanation of enhanced light transmission by a periodical array of holes in a metallic sheet was found to lie in the excitation of surface plasmons on its surface [8, 9], together with the transmission through the holes acting as hollow waveguides below the cut-off of the fundamental mode [10]. This opened several directions for surface plasmon studies. The first one is the study of the light behavior in and around tiny apertures, aiming to increase the field density and to reduce the observation volume for single-molecule spectroscopy [11–13] and biophysical sampling [14]. The second domain is now called plasmonics, with one of the aims being the revival of integrated optics on metallic surfaces [15, 16] and metallic wires [17]. Recent studies have shown that it is possible to compress light within several nanometers in direction transversal to the propagation of the plasmon wave confined between two metallic wires. The second aim of plasmonics is the total control of the plasmon surface wave, by tuning its properties and, in particular, its speed, as necessary for achieving optical delay lines and stronger interaction with matter. It has been shown that the interaction between the surface plasmon and the cavity mode in deep lamellar gratings can significantly modify the plasmon propagation constant [18], but introduces important losses in the visible [19]. In addition, this interaction can create total suppression of the plasmon surface wave (PSW), that can reappear for deeper grooves [20], similar to that observed for sinusoidal grooves almost 20 years ago [21].

As a collateral result of these recent researches on PSW, we observed the revival of plasmonic studies aiming at strong

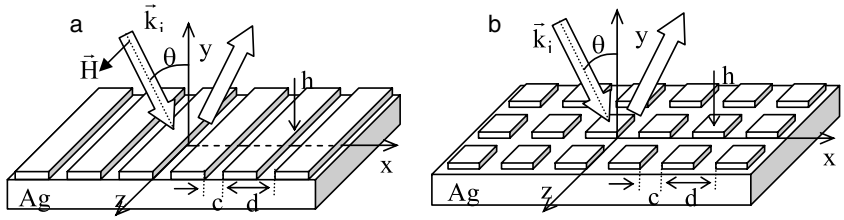

Figure 1. Sketch of lamellar diffraction gratings, together with the coordinate system and notation: grating with 1D (a) and 2D (b) periodicity.

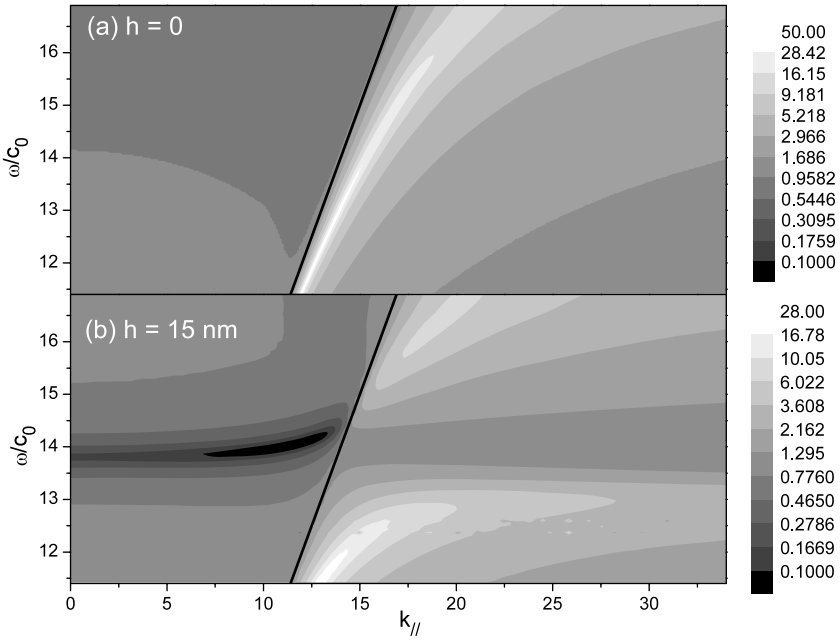

Figure 2. Map of the amplitude of the zeroth reflected order of the diffraction grating presented in figure 1(a) with $d = 60$ nm, $c/d = 1/7$ in the TM polarization as a function of the longitudinal wavenumber $k_\parallel$ and the normalized frequency ω/c_0, both given in μm^{-1}. (a) Planar surface, (b) $h = 15$ nm.

light absorption. The difference from the 1980s is the search for 'less' resonant effects covering larger spectral or/and angular intervals. Almost omnidirectional total absorption has been demonstrated in metallic photonic crystals [22], by using cavity (so-called localized plasmon) resonances in spherical voids [23], or a completely aplasmonic effect in cylindrical rods buried in a metallic layer [24], but although these cavity resonances exhibit a large angular interval, as they are localized in the real space and thus delocalized in the inverse space, the cavities are characterized by a large finesse in the wavelength domain.

The aim of this paper is to study the behavior of PSW for small-pitch shallow (and deep) lamellar metallic gratings, extending the study made in [25] on the absorption properties of such gratings. We show that the grating layer can behave like a high-index lossy dielectric material that can completely cut off the propagation of the PSW and transform its excitation into a Brewster effect. Contrary to the previous studies, where the PSW reappears for deeper grooves [18, 19], the cut-off in our case is definitive, as far as the groove depth exceeds the limit of several nanometers. As a particular consequence, the metamaterial-induced Brewster effect has a non-resonant nature and extends over a large angular and spectral interval. When two-dimensional periodicity (crossed grating) is used, the effect can be extended to unpolarized light.

2. Dispersion behavior and band-gap formation

The structures under study in this paper are shown in figure 1. We consider a lamellar metallic grating having a one-dimensional (a) or two-dimensional periodicity (b). The substrate and the lamellae are made of silver, the period is d, the channel width c and its depth h. The incident light polarization is represented with respect to the plane of incidence, so that TE is the transverse electric with its electric field vector perpendicular to the plane of incidence, and TM, transverse magnetic with its electric field vector lying in the plane of incidence.

The reflectivity properties (amplitude of the zeroth reflected order) of the grating of figure 1(a) are given in figure 2 for the plane silver–air interface ($h = 0$) (a) and for the case of a grating only 15 nm deep (b). The longitudinal wavenumber $k_\parallel = k_x$ is given in inverted microns, ω is the circular frequency, and c_0 the speed of light in vacuo. Commonly,

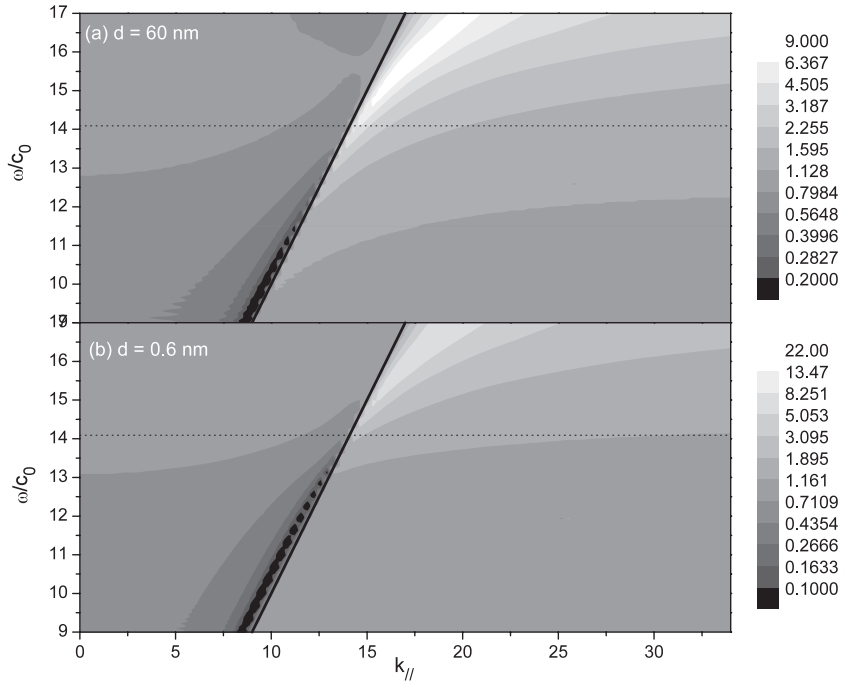

Figure 3. Same as in figure 2 but for an infinite groove depth and two different periods, (a) $d = 60$ nm and (b) $d = 0.6$ nm. The full black line is the light cone and the dotted line corresponds to the value of $\mathrm{Re}(\varepsilon_{\mathrm{eff}}) = -1$ in figure 4.

these maps are used to determine the dispersion relations of the propagation constant k_{p} of the PSW, because the maximum of the reflected amplitude is considered to coincide with the real part of k_{p}. Later, we shall see that this is not always true. What can be observed in figure 2(b) is the formation of a forbidden gap around $\omega/c_0 = 14\ \mu\mathrm{m}^{-1}$, which is accompanied by strong light absorption for real angles of incidence ($k_{\|} > \omega/c_0$).

Due to the lamellar profile, it is possible to model the grating with the use of the eigenvalue/eigenvector technique, as proposed by Moharam and Gaylord [26], improved in 1996 [27, 28] by using the factorization rules in the inverse space, as formulated by Li [29].

Moreover, if we consider very deep lamellae, with the grating depth increasing to infinity [30], we can observe in figure 3(a) that the band-gap is extended to much lower frequencies, and the phenomenon is only slightly affected by the grating period, as observed for a period 100 times shorter in figure 3(b). This fact indicates that the formation of the gap is not due to the Bragg interaction between oppositely propagating PSW. The explanation of this gap can be found in figure 4, which presents the equivalent relative dielectric permittivity $\varepsilon_{\mathrm{eff}} = \bar{\varepsilon}_x$ of the metamaterial substance formed by the grating structure.

The equivalent permittivity is calculated using the homogenization formula for a one-dimensional periodic structure, as explained here. When the grating period is much smaller than the wavelength (as is the case in figure 3(b)) the grating region is equivalent to an anisotropic material with permittivity $\bar{\varepsilon}$. $\bar{\varepsilon}_x$ and $\bar{\varepsilon}_y$ in the case of one-dimensional periodicity can be represented for a lamellar profile in the

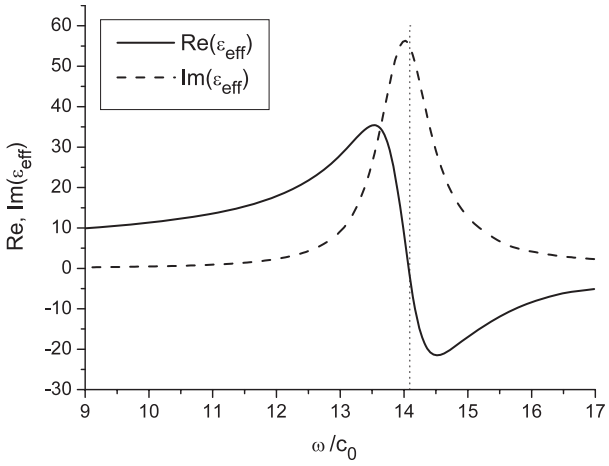

Figure 4. Frequency dependence of the effective relative dielectric permittivity according to equation (1). The dotted line is at $\mathrm{Re}(\varepsilon_{\mathrm{eff}}) = -1$.

form [31–33]:

$$\bar{\varepsilon}_x = \frac{d}{(d-c)/\varepsilon_{\mathrm{m}} + c/\varepsilon_{\mathrm{a}}} \tag{1}$$

$$\bar{\varepsilon}_y = \bar{\varepsilon}_z = \frac{(d-c)}{d}\varepsilon_{\mathrm{m}} + \frac{c}{d}\varepsilon_{\mathrm{a}} \tag{2}$$

where $\varepsilon_{\mathrm{a}} = 1$ is the dielectric permittivity inside the channels, air in our case, and $\varepsilon_{\mathrm{m}} = \varepsilon_{\mathrm{Ag}}$, taken from [34]. The frequency dependence of $\varepsilon_{\mathrm{eff}}$ is presented in figure 4 for $c/d = 1/7$. As can be observed, around 14 $\mu\mathrm{m}^{-1}$, there is a resonance similar to the volume plasmonic resonances for bulk metals close to the electron plasma frequencies. For frequencies lower

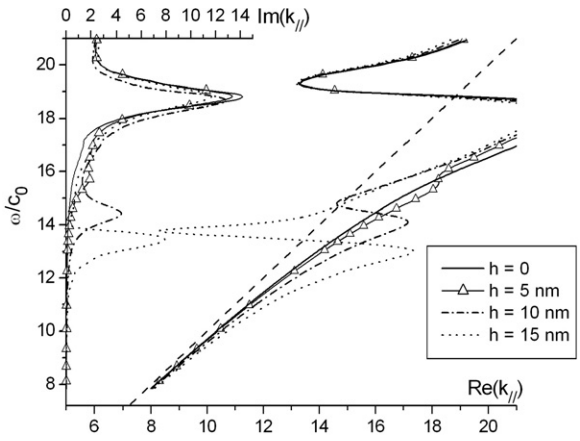

Figure 5. Dispersion relations of the pole of the scattering matrix representing the surface plasmon constant of propagation ($k_\parallel = k_\mathrm{p}$) for the grating given in figure 1(a) with $d = 60$ nm, $c/d = 1/7$, and different groove depths as indicated in the figure. The lower axis and curves on the right are for the real parts of the pole, the upper axis and curves on the left are for the imaginary parts of the pole. All units in $\mu\mathrm{m}^{-1}$. The dashed line is the light cone.

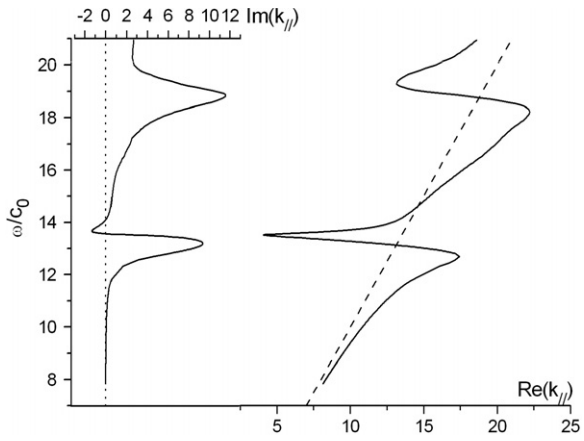

Figure 6. Same as in figure 5, but for $h = 16.5$ nm. The dotted line on the left indicates $\mathrm{Im}(k_\parallel) = 0$.

than 14 $\mu\mathrm{m}^{-1}$, the real part of ε_eff becomes larger than -1, so that the interface with air cannot support the plasmon surface wave. This appears in figure 3 as a transition from a maximum in the reflected amplitude for higher frequencies, into a deep minimum. The transition for short periods (figure 3(b)) appears exactly at the point where $\varepsilon_\mathrm{eff} = -1$ (dotted lines in figures 3 and 4). For larger periods, equation (1) holds only approximately, and the transition frequency in figure 3(a) is a little bit less pronounced.

For the case of two-dimensional periodicity (figure 1(b)), the equivalent permittivity has a different form [35, 36], which gives different values but similar behavior. In the Maxwell-Garnet approximation the form is:

$$\bar{\varepsilon}_x = \bar{\varepsilon}_z = \varepsilon_\mathrm{a}\frac{(1+f)\varepsilon_\mathrm{m} + (1-f)\varepsilon_\mathrm{a}}{(1-f)\varepsilon_\mathrm{m} + (1+f)\varepsilon_\mathrm{a}} \tag{3}$$

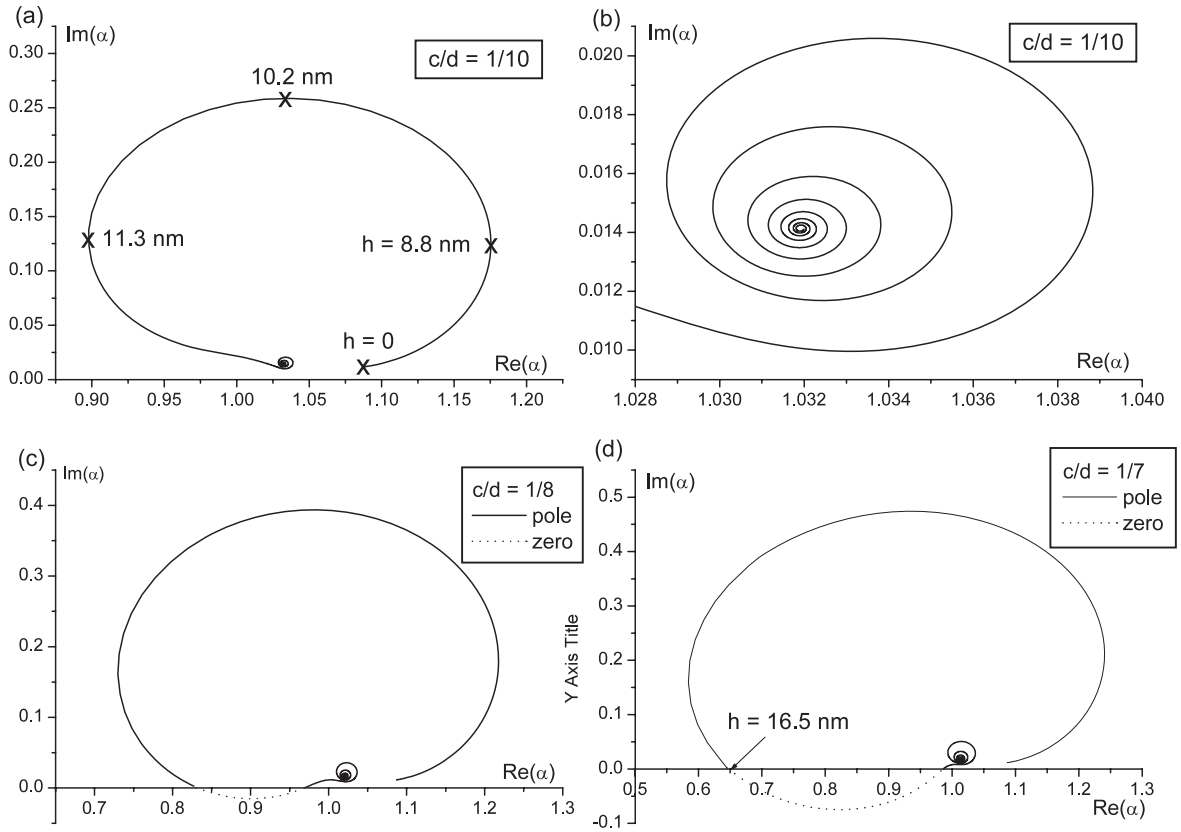

Figure 7. Trajectory of the normalized pole k_p/k_0 of the scattering matrix when the groove depth is varied, obtained for different groove widths. (a) $c/d = 1/10$, (b) zoom of (a) for larger h values, (c) $c/d = 1/8$, (d) $c/d = 1/7$. Solid line, pole, dashed line, zero of the zeroth reflected order.

$$\bar{\varepsilon}_y = f\varepsilon_m + (1-f)\varepsilon_a \tag{4}$$

where

$$f = \left(1 - \frac{c}{d}\right)^2 \tag{5}$$

is the filling factor.

As already mentioned, the reflectivity properties do not always represent the PSW propagation constant very well. This is more pronounced when the imaginary part of k_p is large, which would be the case when ε_{eff} has a large imaginary part (see figure 4 close to 14 μm^{-1}). Much more precise are the results obtained by the pole-searching procedure applied in the complex $k_\parallel$ plane. Figures 5 and 6 present the dispersion relations for the real and imaginary parts of the poles of the scattering matrix of the system for different groove depths, starting from a plane silver–air interface ($h = 0$). For a flat surface, the real part of the pole follows the maximum in the reflectivity observed in figure 2(a) quite well. In addition, one sees, in figure 5, the electron plasma resonance near 19 μm^{-1} (i.e., a wavelength of 330 nm), which gives a high-frequency cut-off of the PSW.

With the presence of the grating ($h = 5$ nm), a spike appears in the real part close to 15 μm^{-1}, accompanied by an increase of the imaginary part of $k_\parallel$. This behavior can be understood in view of substituting the grating with a thin anisotropic layer, having a metamaterial-induced plasmon cut-off close to 14 μm^{-1} (figure 4). Its influence grows with h, so that when $h = 15$ nm, the real part of the pole goes inside the light cone and the PSW disappears, thus explaining the band-gap observed in figure 2(b).

Even more surprising is the behavior of the pole for $h = 16.5$ nm (figure 6), where there is a region with a negative imaginary part of the pole. There is no physical contradiction (there are no gains), because at the same time the real part lies inside the light cone and the PSW does not propagate. In fact, the pole in that case is transformed into a zero of the zeroth reflected order amplitude, as explained in the next section, so that the PSW is transformed into the Brewster effect, which explains the increase of absorption for real incident angles close to 14 μm^{-1} in figure 2(b).

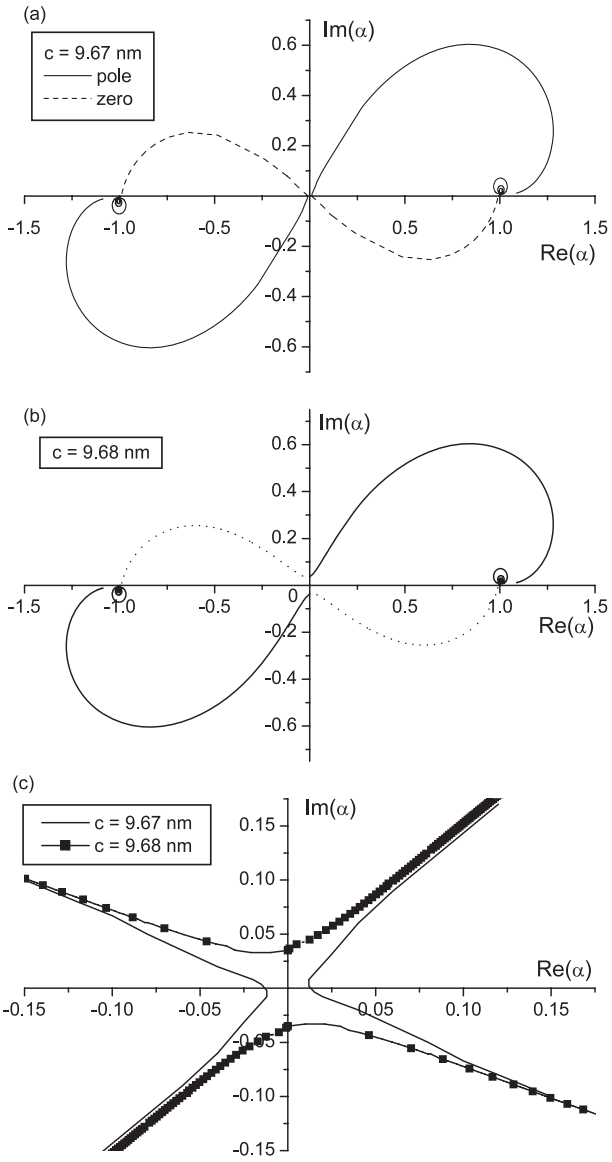

Figure 8. Same as in figure 7, but for two close groove width values, (a) $c = 9.67$ nm, (b) $c = 9.68$ nm. (c) zoom close to the origin of the two curves (no distinction is made here between the pole and the zero).

3. Pole/zero trajectories in the complex $k_\parallel$-plane and total light absorption

In section 2 we present the behavior of the pole as a function of the wavelength at fixed groove depth, which gives its dispersion properties. Another way of presenting the PSW propagation constant is to fix the wavelength and study the trajectory of the propagation constant in the complex plane when the groove depth is varied. Figure 7 presents the trajectory of the normalized propagation constant $\alpha = k_p/k_0$, where $k_0 = 2\pi/\lambda$, for three different groove widths and at $\lambda = 457$ nm ($\omega/c_0 = 13.75\ \mu m^{-1}$).

At $h = 0$, whatever the groove width, the starting point of the trajectory is the same, corresponding to α at the plane silver–air interface. The increase of groove depth leads to an increase of the imaginary part of α, as the losses inside the grating region increase. More interesting is that for groove channel values lying between $0 < c/d < 1/5$, there is a turning point of the trajectory close to $h = 10$ nm, so that for deeper grooves the imaginary part of α diminishes. However, when this happens, the imaginary part of α is smaller than 1, so that the solution is not localized close to the grating surface, because the real part of α corresponds to the sine of the angle of reflection. When $\mathrm{Re}(\alpha) < 1$, the pole of the scattering matrix corresponds to a Fabry–Perot lossy resonance, rather than to a PSW. For narrow grooves ($c/d = 1/10$, figure 7(a)), the trajectory of α lies inside the first quadrant, and tends in a spiral towards the value of α that corresponds to infinitely deep grooves (figure 7(b)). However, with an increase of the channel width, inside a certain interval of h, the trajectory of α crosses the real axis and its imaginary part becomes negative. However, this does not mean that we obtain Fabry–Perot resonance with gain, as already mentioned with respect

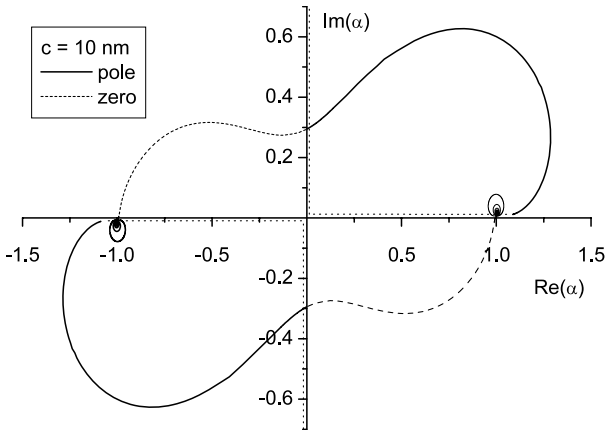

Figure 9. Same as in figure 7, but for $c/d = 1/6$.

to figure 6. In fact, there is a cut in the complex plane that starts from the branching point $\alpha = 1$, goes along the real axis down to the origin, then comes up to infinity along the imaginary axis. A symmetrical cut exists in the third quadrant of the complex α-plane with a branch point at -1. This cut is due to the necessity to chose the sine of the square root in determining the normalized wavenumber β of the reflected zeroth order in air along the vertical y-axis, given by:

$$\beta = \pm\sqrt{1-\alpha^2}. \tag{6}$$

This wavenumber has to have a nonnegative imaginary part in order to ensure that the diffracted wave in the cladding does not diverge when going away from the surface; i.e., when crossing the real α-axis, it is necessary to invert the choice of the sign in equation (6), which is expressed mathematically by a cut in the complex α-plane.

When the pole of the scattering matrix crosses this cut, it is transformed into a zero of the zeroth reflected order. Interested readers can find details in [37–40], but here is a brief idea how to explain this simply. Let us consider a single plane interface between two media, numbered with 1 and 2. The Fresnel reflection coefficient is given by:

$$r_{\mathrm{TM}} = \frac{\beta_1/\varepsilon_1 - \beta_2/\varepsilon_2}{\beta_1/\varepsilon_1 + \beta_2/\varepsilon_2}. \tag{7}$$

If, for a given value of α and choice of the sign of the square root in equation (6), there is a zero of the denominator in equation (7), this zero corresponds to a pole of r_{TM}, called PSW. The change of the choice of the sign in (6) that happens when crossing the cut, will permute the nominator and denominator in equation (7), transforming the pole into a zero of r_{TM}.

Returning to figure 7, the trajectory of the zero is represented by a dashed line. The crossing point with the real axis corresponds to a zero in reflection for real incident angles, i.e. total light absorption, provided the period is sufficiently short to not allow diffraction orders other than zero. Similar behavior was found 20 years ago in the case of sinusoidal profiles, which required somewhat deeper grooves [41, 42].

With an increase of the groove width, the loop of the trajectory becomes larger and starts to pass near the origin. There is a symmetrical loop that starts from the propagation constant of the surface plasmon propagating in the opposite direction. When these two trajectories tend to cross for some groove depth values and wider grooves (figure 8), there is a repulsion between the curves (sometimes called anticrossing), due to the interaction of the two solutions. This leads to the exchange of the curves between the two poles, as seen in detail in figure 8(c) for two consecutive, very close, values of c. A further increase of c leads to a separation of the exchanged curves, as seen in figure 9 for $c/d = 1/6$.

As discussed above, the crossing of the trajectory and the real axis means total absorption of incident light. Because of its non-resonant nature (the pole has disappeared and transformed into a zero), one can expect a large angular and spectral interval with low reflectivity. However, this can be expected in only one (TM) polarization. In order to obtain strong absorption in unpolarized light, it is possible to use a crossed grating that has a periodicity in two directions (figure 1(b)), so that one polarization can be absorbed due to the periodicity in one

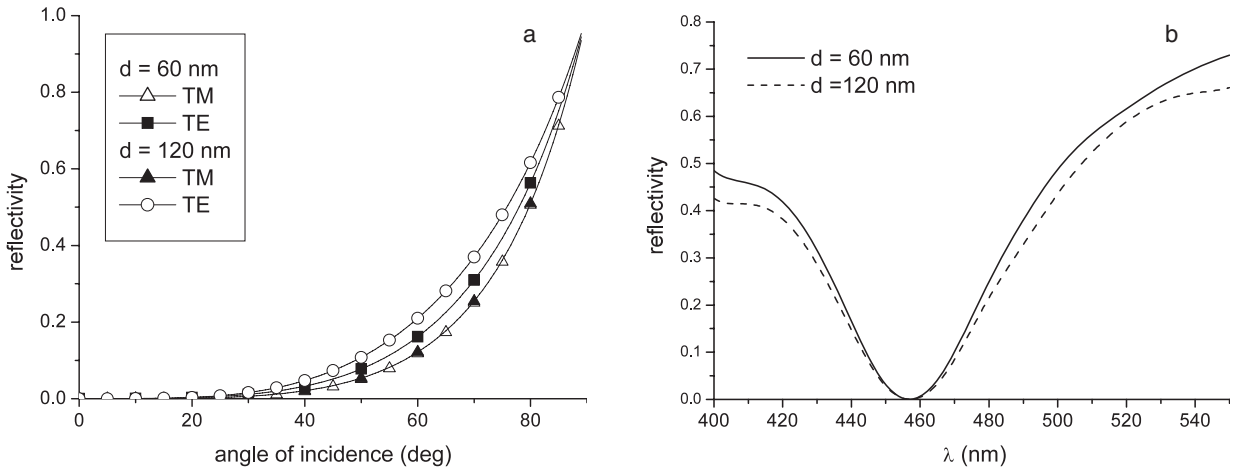

Figure 10. Angular (a) and spectral (b) dependence of the reflectivity of two gratings of type given in figure 1(b) with $d = 60$ nm, $c = 15$ nm, and $h = 21.5$ nm, and $d = 120$ nm, $c = 30$ nm, and $h = 27.5$ nm, respectively. The wavelength in (a) is 457 nm, and the incidence in (b) is normal; the polarizations are given in (a), and in (b) the light is unpolarized.

direction, while the other polarization can be absorbed through the periodicity in the other direction. We have optimized the grating parameters c and h for two different periods $d = 60$ and 120 nm using Fourier-modal method [43], which represents an extension to the 2D periodical case. The angular dependence of the reflectivity at $\lambda = 457$ nm is presented in figure 10(a) for the following parameters, $d = 60$ nm, $c = 15$ nm, and $h = 21.5$ nm, and $d = 120$ nm, $c = 30$ nm, and $h = 27.5$ nm. The reflectivity remains lower than 5% within an angular interval from $-40°$ to $40°$. At normal incidence, the spectral width at a half-height is larger than 80 nm, as seen in figure 10(b).

4. Conclusion

We have demonstrated that even very shallow short-period lamellar diffraction gratings can completely cut the propagation of a plasmon surface wave on a metal–air interface, by forming an effective metamaterials equivalent to a lossy high-index dielectric layer, thus transforming the surface plasmon resonance into a Brewster effect that can lead to strong light absorption over a large range of angles of incidence and wavelength. The question remains open whether, in larger-period grating, this transformation is accompanied by a formation of a localized plasmon wave or not.

References

[1] Wood R W 1902 On a remarkable case of uneven distribution of light in a diffraction grating spectrum *Phil. Mag.* **4** 396–402

[2] Fano U 1941 The theory of anomalous diffraction gratings and of quasi-stationary waves on metallic surfaces (Sommerfeld's waves) *J. Opt. Soc. Am.* **31** 213–22

[3] Hessel A and Oliner A A 1965 A new theory of Wood's anomalies on optical gratings *Appl. Opt.* **4** 1275–97

[4] Hutley M C and Maystre D 1976 Total absorption of light by a diffraction grating *Opt. Commun.* **19** 431–6

[5] McPhedran R C, Derrick G H and Botten L C 1980 Theory of crossed gratings *Electromagnetic Theory of Gratings* ed R Petit (Berlin: Springer)

[6] Popov E, Enoch S, Tayeb G, Nevière M, Gralak B and Bonod N 2004 Enhanced transmission due to non-plasmon resonances in one and two-dimensional gratings *Appl. Opt.* **43** 999–1008

[7] Mashev L B, Popov E K and Loewen E G 1988 Total absorption of light by a sinusoidal grating near grazing incidence *Appl. Opt.* **27** 152–4

[8] Ebbesen T W, Lezec H J, Ghaemi H F, Thio T and Wolff P A 1998 Extraordinary optical transmission through subwavelength hole arrays *Nature* **391** 667–9

[9] Popov E, Nevière M, Enoch S and Reinisch R 2000 Theory of light transmission through subwavelength periodic hole arrays *Phys. Rev.* B **62** 16100–8

[10] Enoch S, Popov E, Nevière M and Reinisch R 2002 Enhanced light transmission by hole arrays *J. Opt. A: Pure Appl. Opt.* **4** S83–7

[11] Levene M J, Korlach J, Turner S W, Foquet M, Craighead H G and Webb W W 2003 Zero-mode waveguides for single-molecule analysis at high concentrations *Science* **299** 682–6

[12] Genet C and Ebbesen T W 2007 Light in tiny holes *Nature* **445** 39

[13] Craighead H 2006 Future lab-on-a-chip technologies for interrogating individual molecules *Nature* **442** 387–93

[14] Samiee K T, Foquet M, Guo L, Cox E C and Craighead H G 2005 λ-repressor oligomerization kinetics at high concentrations using fluorescence correlation spectroscopy in zero-mode waveguides *Biophys. J.* **88** 2145–53

[15] Barnes W L, Dereux A and Ebbesen T W 2003 Surface plasmon subwavelength optics *Nature* **424** 824–29

[16] Ozbay E 2006 Plasmonics: merging photonics and electronics at nanoscale dimensions *Science* **311** 189

[17] Conway J A, Sahni S and Szkopek T 2007 Plasmonic interconnects versus conventional interconnects: a comparison of latency, crosstalk and energy costs *Opt. Express* **15** 4474–84

[18] Pendry J B, Martin-Moreno L and Garcia-Vidal F J 2004 Mimicking surface plasmons with structured surfaces *Science* **305** 847–8

[19] Popov E, Bonod N and Enoch St 2007 Non-Bloch plasmonic stop-band in real-metal gratings *Opt. Express* **15** 6241–50

[20] Garcia-Vidal F J, Sánchez-Dehesa J, Dechelette A, Bustarret E, López-Rios T, Fournier T and Pannetier B 1999 Localized surface plasmons in lamellar metallic gratings *J. Lightwave Technol.* **17** 2191–5

[21] Popov E, Tsonev L and Maystre D 1990 Losses of plasmon surface wave on metallic grating *J. Mod. Opt.* **37** 379–87

[22] Veronis G, Dutton R W and Fan S H 2005 Metallic photonic crystals with strong broadband absorption at optical frequencies over wide angular range *J. Appl. Phys.* **97** 093104

[23] Teperik T V, García De Abajo F J, Borisov A G, Abdelsalam M, Bartlett P N, Sugawara Y and Baumberg J J 2008 Omnidirectional absorption in nanostuctured metal surfaces *Nat. Photon.* **2** 299–301

[24] Bonod N and Popov E 2008 Total light absorption in a wide range of incidence by nanostructured metals without plasmons *Opt. Lett.* **33** 2398–400

[25] Le Perchec J, Quémerais P, Barbara A and López-Rios T 2008 Why metallic surfaces with grooves a few nanometers deep and wide may strongly absorb visible light *Phys. Rev. Lett.* **100** 066408

[26] Moharam M G and Gaylord T K 1982 Rigorous coupled-wave analysis of dielectric surface-relief gratings *J. Opt. Soc. Am.* **72** 1385–92

[27] Lalanne P and Morris G M 1996 Highly improved convergence of the coupled-wave method for TM polarization *J. Opt. Soc. Am.* A **13** 779–84

[28] Granet G and Guizal B 1996 Efficient implementation of the coupled-wave method for metallic gratings in TM polarization *J. Opt. Soc. Am.* A **13** 1019–23

[29] Li L 1996 Use of Fourier series in the analysis of discontinuous periodic structures *J. Opt. Soc. Am.* A **13** 1024–35

[30] Lalanne P, Rodier J C and Hugonin J P 2005 Surface plasmons of metallic surfaces perforated by nanohole arrays *J. Opt. A: Pure Appl. Opt.* **7** 422–6

[31] McPhedran R, Botten L, Craig M, Nevière M and Maystre D 1982 Lossy lamellar gratings in the quasistatic limit *Opt. Acta* **29** 289–312

[32] Bouchitte G and Petit R 1985 Homogenization techniques as applied in the electromagnetic theory of gratings *Electromagnetics* **5** 17–36

[33] Popov E and Enoch S 2007 Mystery of the double limit in homogenisation of finitely or perfectly conducting periodic structures *Opt. Lett.* **32** 3441–3

[34] http://www.luxpop.com/

[35] Maxwell-Garnet J C 1904 Colors in metal glasses and in. metallic films *Phil. Trans. R. Soc.* A **203** 385–420

[36] Yaghjian D 1980 Electric dyadic Green's functions in the source region *Proc. IEEE* **68** 248–63

[37] Hessel A and Oliner A A 1986 Wood's anomaly effects on gratings of large amplitude *Opt. Commun.* **59** 327

[38] Maystre D 1982 General study of grating anomalies from electromagnetic surface modes *Electromagnetic Surface Modes* ed A D Boardman (New York: Wiley) chapter 7

[39] Nevière M 1980 The homogeneous problem *Electromagnetic Theory of Gratings* ed R Petit (Berlin: Springer) chapter 5
[40] Popov E 1993 Light diffraction by relief gratings: macro and microscopic point of view *Progress in Optics* ed E Wolf (Amsterdam: Elsevier) chapter 2, pp 139–87
[41] Mashev L, Popov E and Loewen E 1989 Brewster effect for deep metallic gratings *Appl. Opt.* **28** 2538–41
[42] Popov E, Mashev L and Loewen E 1989 Total absorption of light by metallic grating in grazing incidence a connection in the complex plane with other anomalies *Appl. Opt.* **28** 970–5
[43] Li L 1997 New formulation of the Fourier modal method for crossed surface-relief gratings *J. Opt. Soc. Am.* A **14** 2758–67